Hydrology and Earth System Sciences

Supporting Information for

Role of Forest Stand Structure in Groundwater Storage Decline in the Three-North Shelterbelt Forest Region, China

Shu Luo[1], Longhuan Wang[1,2*], Jia Wang[1*], Binghao Jia[2], Rui Han[3], Shaodong Huang[1], Panfei Fang[1], Yujie Li[1], Chu Chu[1], Jianwen Zhang[1]

[1]Beijing Key Laboratory of Precision Forestry, Beijing Forestry University, Beijing, 100083, China

[2]State Key Laboratory of Earth System Numerical Modeling and Application, Institute of Atmospheric Physics, Chinese Academy of Sciences, Beijing, 100029, China

[3]Institute of Environment and Sustainable Development in Agriculture, Chinese Academy of Agricultural Sciences, 100081, Beijing, China

Contents of this file

Text S1

Contribution analysis of SMSA

To identify the dominant hydrological components driving terrestrial water storage anomalies (TWSA) variability, we quantified the relative contribution of each available water-storage component using the component contribution ratio (CCR) method (Kim et al., 2009).

For each water storage component S_i, the mean absolute deviation (MAD_{S_i}) from its long-term mean was first calculated as:

$$MAD_{S_i} = \frac{1}{N}\sum_{i=1}^{N}|S_i - \bar{S}_i|, \quad (1)$$

where S_i is the water-storage component, $\bar{S}_i$ is the long-term mean of S_i, and N is the number of months during the study period. The CCR was then calculated as:

$$CCR_{S_i} = \frac{MAD_{S_i}}{\sum_{i=1}^{M} MAD_{S_i}}, \quad (2)$$

where CCR_{S_i} represents the relative contribution of component S_i to the temporal variability of TWSA, and M is the total number of components.

Text S2

Evaluation of SMSA using Satellite-derived soil moisture data

We further used the European Space Agency Climate Change Initiative (ESA CCI) soil moisture product as an independent reference (Dorigo, W. et al., 2025). It was used to evaluate surface soil moisture from the Global Land Data Assimilation System (GLDAS) and the fifth generation of European ReAnalysis (ERA5) (Ling et al., 2021). ESA CCI data were obtained from the ESA Climate Change Initiative Soil Moisture project (https://data.ceda.ac.uk/neodc/esacci/soil_moisture/data). ERA5 soil moisture data were provided by the Copernicus Climate Data Store (https://cds.climate.copernicus.eu/datasets), at a spatial resolution of 0.25° (Hersbach, H. et al., 2023). Since ESA CCI dataset mainly reflects near-surface soil moisture, this comparison was used to assess the consistency of the surface soil moisture component, rather than to directly validate the soil moisture storage anomalies (SMSA).

Daily ESA CCI soil moisture data were first aggregated into monthly averages for the period from January 2003 to December 2023. The surface soil moisture from ERA5 was derived from its top soil layer (0–7 cm), whereas GLDAS surface soil moisture corresponds to the 0–10 cm layer. Since GLDAS soil moisture is provided as water-equivalent depth, it was converted to volumetric soil moisture before comparison with ESA CCI (Guan et al., 2023):

$$\theta_{GLDAS} = \frac{SM_{GLDAS}}{D \times 1000}, \quad (3)$$

where θ_{GLDAS} is the GLDAS volumetric soil moisture in $m^3\ m^{-3}$, SM_{GLDAS} is the GLDAS soil water

storage in kg m^{-2} or mm, and $D$is the soil layer thickness in metres. ERA5 and GLDAS were spatially resampled via linear interpolation to match the resolution of the ESA CCI dataset.

The consistency assessment was conducted at three levels. First, regional mean time series were calculated using area weights proportional to the cosine of latitude:

$$\bar{\theta}(t)=\frac{\sum_{i=1}^{n}\omega_i\theta_i(t)}{\sum_{i=1}^{n}\omega_i}, \quad (4)$$

where $\theta_i(t)$denotes soil moisture at grid cell $i$and time t, and $\omega_i = \cos(\mathrm{lat}_i)$ is the corresponding area weight. Second, ERA5 and GLDAS values were paired with ESA CCI values at the same grid cells and months. All available paired monthly values were pooled to evaluate the overall agreement across the study region. Finally, correlation coefficients and root mean square error (RMSE) were calculated at each grid cell using the monthly time series to examine spatial differences in product performance.

For the paired samples, the correlation coefficient and RMSE were calculated as follows:

$$R=\frac{\sum_{j=1}^{N}(X_j-\bar{X})(Y_j-\bar{Y})}{\sqrt{\sum_{j=1}^{N}(X_j-\bar{X})^2}\sqrt{\sum_{j=1}^{N}(Y_j-\bar{Y})^2}}, \quad (5)$$

$$RMSE=\sqrt{\frac{1}{N}\sum_{j=1}^{N}(Y_j-X_j)^2}, \quad (6)$$

where $X_j$represents ESA CCI soil moisture, $Y_j$represents soil moisture from ERA5 or GLDAS, and $N$is the number of valid paired samples.

Text S3

Evaluation of SMSA based on in-situ observations

To complement the validation of SMSA, GLDAS and ERA5 soil moisture products were evaluated against in situ soil moisture observations from the China Meteorological Administration (CMA) for 2012–2017 (Wang and He, 2015; Zeng et al., 2021, 2024, 2025). This comparison provides an additional ground-based assessment of the soil moisture products used to estimate SMSA.

Daily CMA soil moisture observations were first aggregated into monthly means. The corresponding GLDAS and ERA5 values were then extracted from the nearest grid cell for each station.

The evaluation was conducted for both surface and root-zone soil moisture. For surface soil moisture, CMA observations and GLDAS both used the 0–10 cm layer. ERA5 used the first soil layer, corresponding to 0–7 cm. For 0–100 cm root-zone soil moisture, CMA observations were directly obtained from the corresponding layer of the station dataset. GLDAS root-zone soil moisture was derived by summing soil water storage across the 0–10 cm, 10–40 cm, and 40–100 cm layers, followed by division by 1000 mm (Zhang et al., 2022). ERA5 root-zone soil moisture was calculated as a thickness-weighted mean:

$$\theta_{ERA5}=\frac{7\theta_1+21\theta_2+72\theta_3}{100}, \quad (7)$$

where θ_1, θ_2, and θ_3 denote the volumetric soil moisture of ERA5 in the 0–7, 7–28, and 28–100 cm layers, respectively.

For each station, the correlation coefficient and RMSE were calculated between observed and modelled monthly soil moisture series. The overall performance of each product was then described using the averaged correlation and RMSE across all stations:

$$\overline{R}=\frac{1}{K}\sum_{k=1}^{K} R_k, \tag{8}$$

$$\overline{RMSE}=\frac{1}{k}\sum_{k=1}^{k} RMSE_k, \tag{9}$$

where K is the total number of stations, and R_k and $RMSE_k$ are the correlation coefficient and RMSE at station k, respectively.

Test S4

Uncertainty analysis

To assess the influence of Gravity Recovery and Climate Experiment (GRACE) product selection on groundwater storage anomalies (GWSA) estimates, we separately calculated GWSA using Center for Space Research mascon solution (CSR) and Jet Propulsion Laboratory (JPL) TWSA products via the mass balance approach:

$$GWSA_p(t)=TWSA_p(t)-SWA(t)-SMSA(t)-CWSA(t) \tag{10}$$

where p denotes either the CSR or JPL product. The hydrological storage components subtracted from TWSA, including snow water storage anomalies (SWA), soil moisture storage anomalies (SMSA), and canopy water storage anomalies (CWSA), were kept identical in the two calculations. The uncertainty in regional GWSA trend (σ_{trend})was estimated from two components: the uncertainty related to differences between GRACE products ($\sigma_{products}$)and the uncertainty associated with linear fitting ($\sigma_{fitting}$) (Scanlon et al., 2018). A Monte Carlo simulation was used to estimate $\sigma_{products}$ (Zhao et al., 2021). At each time step, the mean value and one standard deviation of the GWSA estimates from the different GRACE products were calculated and used as the mean (μ) and standard deviation (σ) of a Gaussian distribution, $N(\mu,\sigma^2)$. An ensemble of 1000 regional GWSA time series was then generated from this distribution, and linear trends were calculated for all ensemble members. $\sigma_{products}$ was defined as one standard deviation of these 1000 trend estimates. The fitting uncertainty ($\sigma_{fitting}$) was represented by the standard error of the linear trend fitted to the mean regional GWSA time series. The total uncertainty in the regional GWSA trend was calculated as:

$$\sigma_{trend}=\sqrt{\sigma_{products}^2+\sigma_{fitting}^2}, \tag{11}$$

Figures

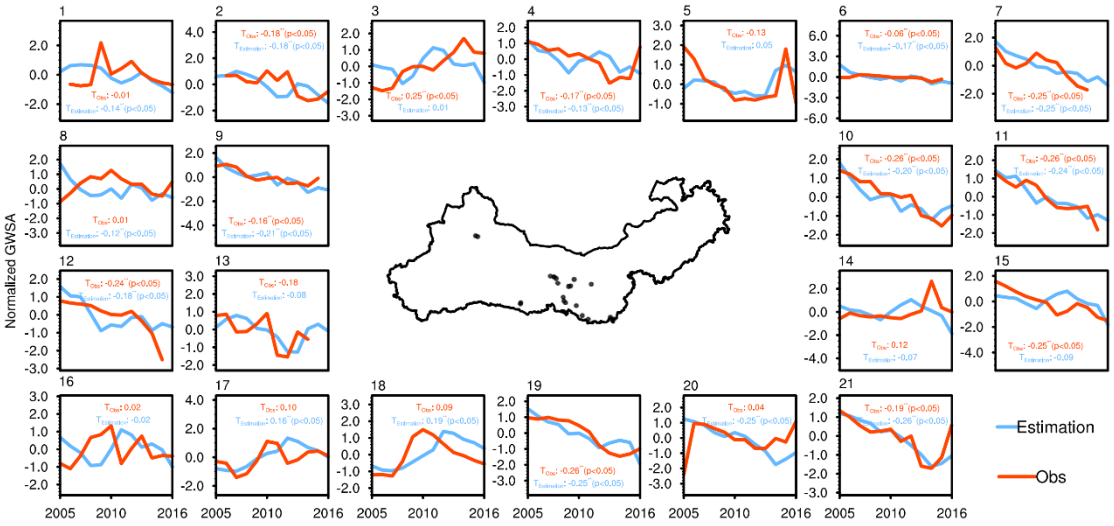

Figure S1 Comparison of estimated (blue lines) and observed (red lines) GWSA at 21 groundwater monitoring wells during 2005–2016. The central map shows the spatial distribution of monitoring wells within the TNSFR. T_{Obs} and $T_{Estimation}$ represent the linear trends of observed and estimated GWSA, respectively. ** indicates statistical significance at $p < 0.05$.

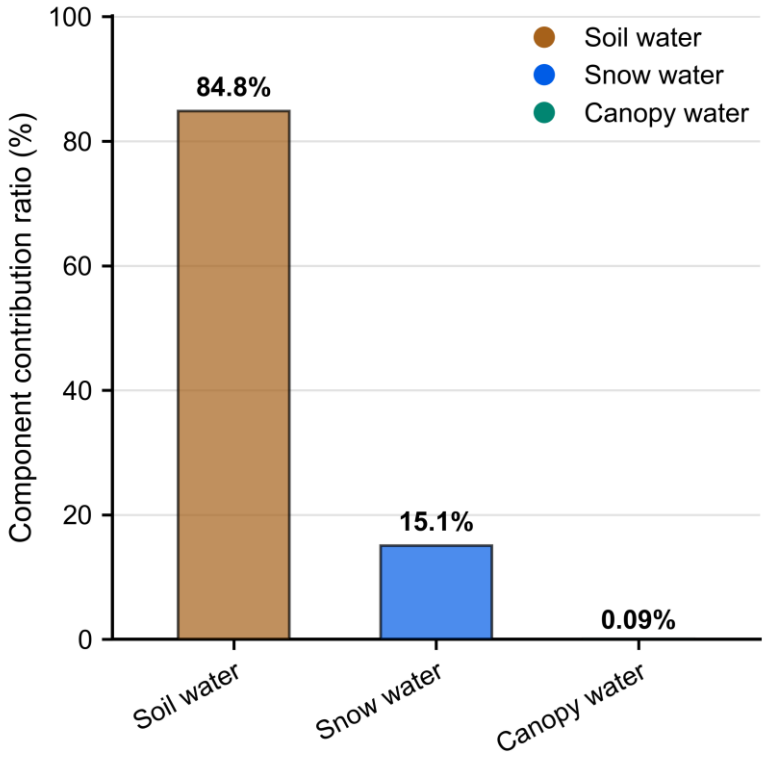

Figure S2 CCR of GLDAS water storage components contributing to temporal variations in TWSA.

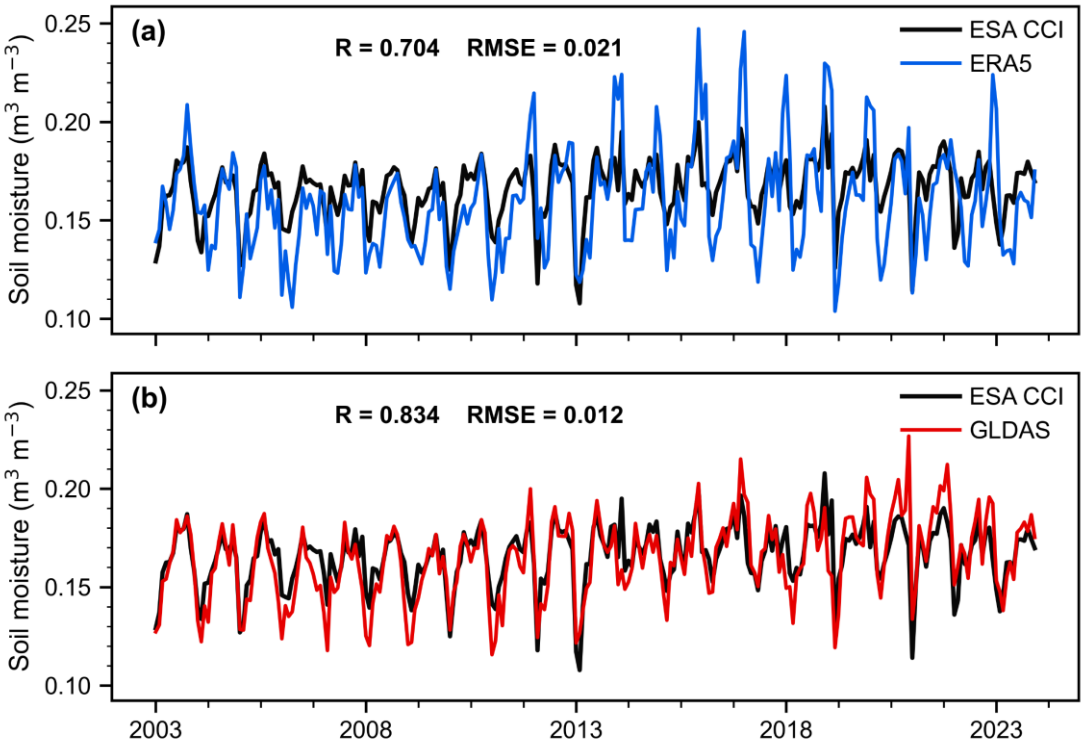

125 **Figure S3** Comparison of regional mean monthly soil moisture from ESA CCI, ERA5, and GLDAS during 2003–2023. The black lines denote ESA CCI soil moisture, while the blue and red lines denote ERA5 and GLDAS, respectively.

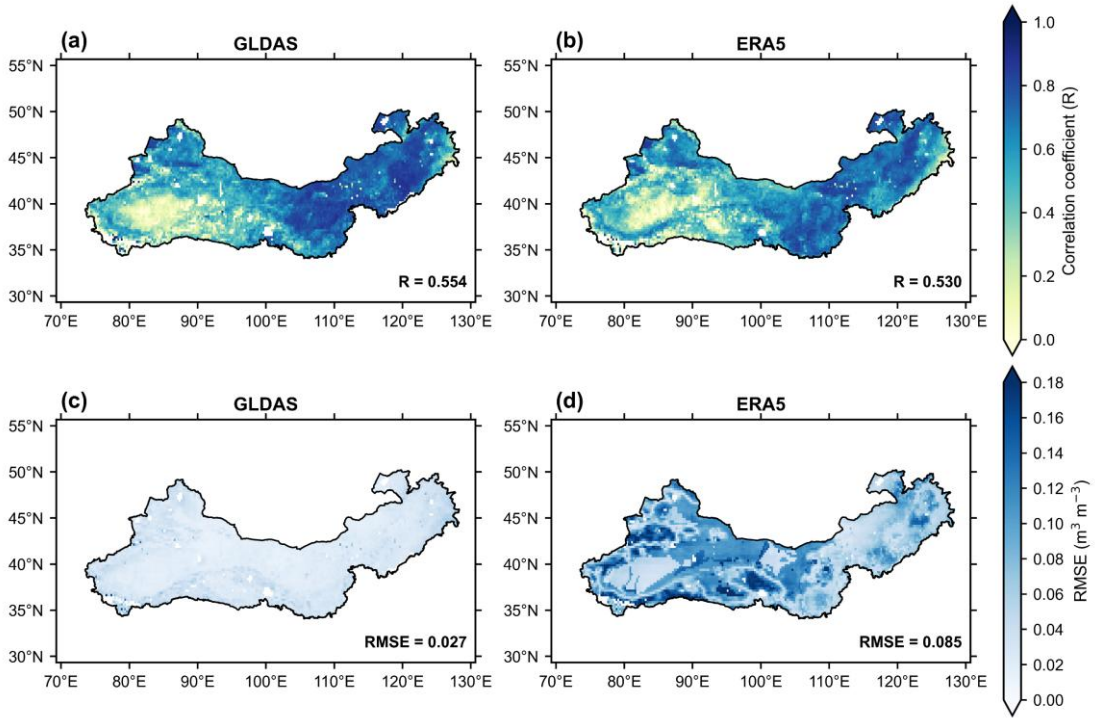

Figure S4 Comparison of GLDAS and ERA5 soil moisture with ESA CCI over the study region.

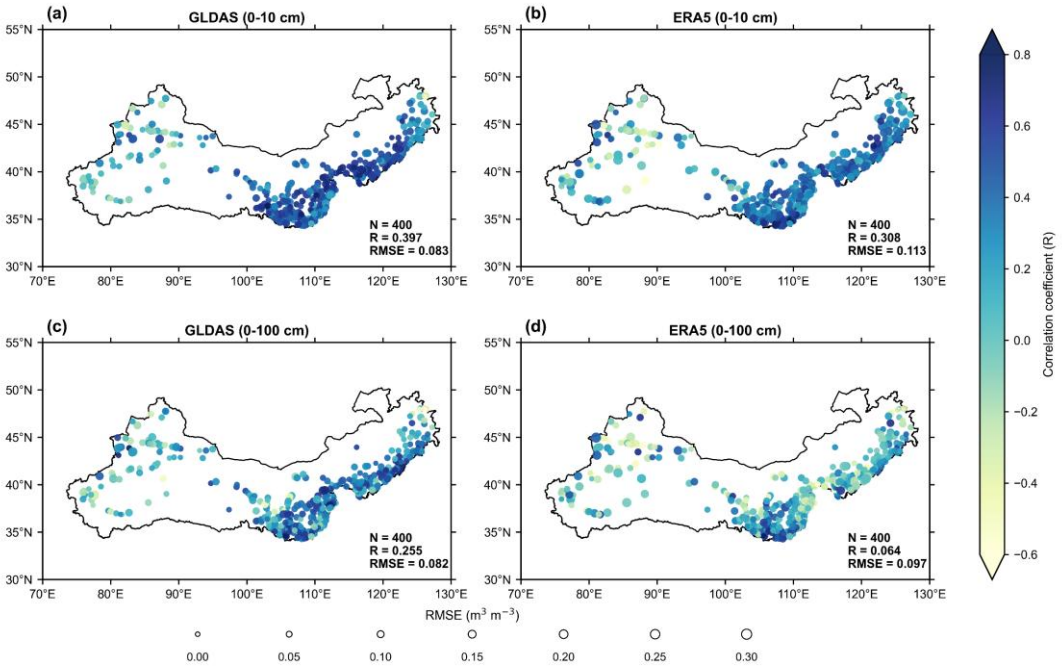

Figure S5 Comparison of GLDAS and ERA5 soil moisture with station observations for (a) GLDAS 0–10 cm, (b) ERA5 0–10 cm, (c) GLDAS 0–100 cm, and (d) ERA5 0–100 cm soil moisture. Colors denote the correlation coefficient (R), and circle sizes indicate RMSE ($m^3\ m^{-3}$).

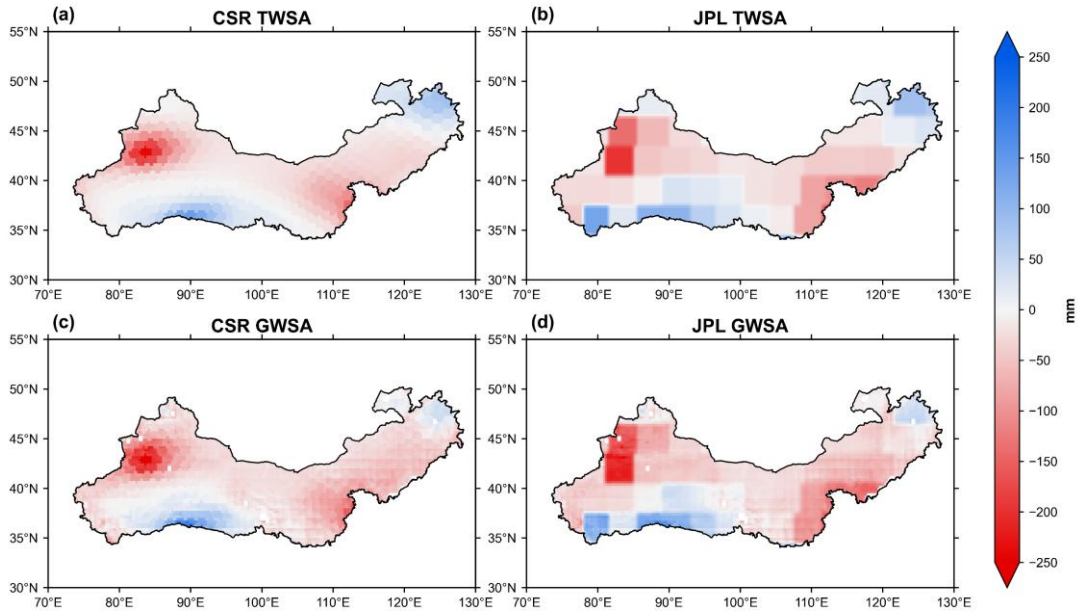

Figure S6 Comparison of the multi-year mean TWSA and GWSA derived from CSR and JPL GRACE products over the study region.

140

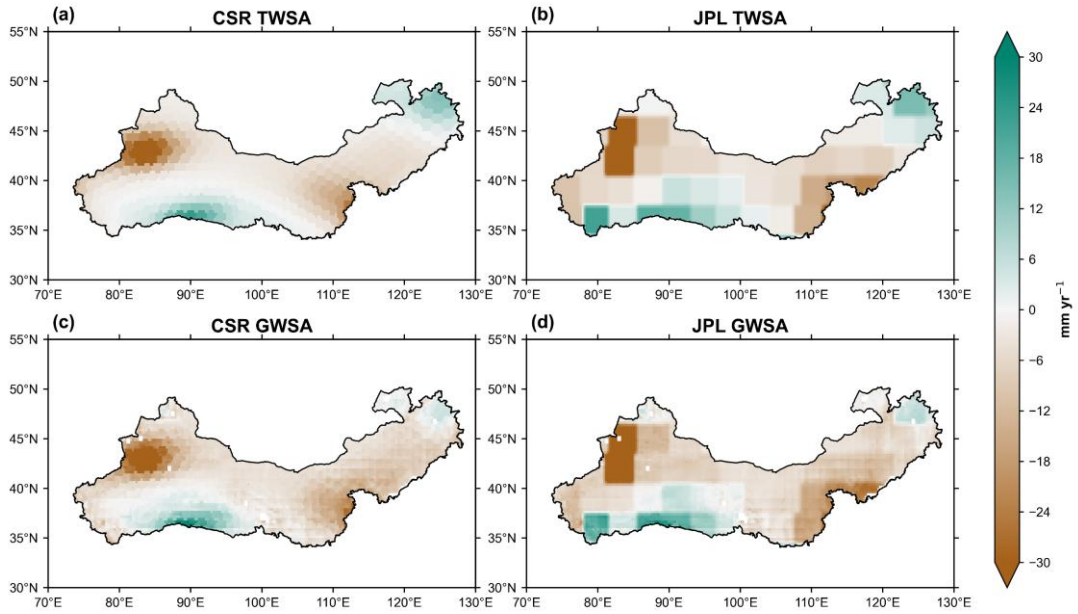

Figure S7 Comparison of TWSA and GWSA trends derived from CSR and JPL GRACE products over the study region.

TablesS1

Table S1. Datasets Used for GWSA Estimation and Assessment.

Data	Resolution	Periods	Source
TWS	CSR-M JPL-M 0.25°	2003-2023	https://www2.csr.utexas.edu/grace/RL06_mascons.html https://grace.jpl.nasa.gov/data/get-data/jpl_global_mascons/
canopy water, snow water and soil water	0.25°	2003-2023	(Rodell et al., 2004)
ERA5	0.25°	2003-2023	https://cds.climate.copernicus.eu/datasets
ESA CCI	0.25°	2003-2023	https://data.ceda.ac.uk/neodc/esacci/soil_moisture/data
Soil moisture observation	Site	2012-2017	China Meteorological Administration
Precipitation and temperature	1km	2003-2023	(Peng et al., 2019)
Evapotranspiration	0.1°	2003-2023	(Miralles et al., 2025)
Human activities GDP Irrigation area population coal production	-	2003-2023	Natural Bureau of Statistics
Groundwater table depth	Site	2005-2016	Geological Environment Monitoring Institute of China Geological Survey
AI	30 arc-seconds	1970-2000	(Zomer et al., 2022)
NDVI	0.1°	2003-2024	https://modis.gsfc.nasa.gov/
Forest Inventory data	Plot	The 9th National Forest Inventory	National Forestry and Grassland Administration
GDE	30m	2015-2020	(Rohde et al., 2024)
CLCD	30m	2003-2023	(Yang and Huang, 2021)

Data Availability Statement

All the data sources have been stated in the manuscript.

References

Dorigo, W., Preimesberger, W., Hahn, S., Van der Schalie, R., De Jeu, R., Kidd, R., Rodriguez-Fernandez, N., Hirschi, M., Stradiotti, P., Frederikse, T., Gruber, A., and Duchemin, D.: ESA Soil Moisture Climate Change Initiative (Soil_Moisture_cci): Version 09.2 data collection, 2025.

Guan, Y., Gu, X., Slater, L. J., Li, J., Kong, D., and Zhang, X.: Spatio-temporal variations in global surface soil moisture based on multiple datasets: Intercomparison and climate drivers, J. Hydrol., 625, 130095, https://doi.org/10.1016/j.jhydrol.2023.130095, 2023.

Hersbach, H., Bell, B., Berrisford, P., Biavati, G., Horányi, A., Muñoz Sabater, J., Nicolas, J., Peubey, C., Radu, R., Rozum, I., Schepers, D., Simmons, A., Soci, C., Dee, D., and Thépaut, J.-N.: ERA5 monthly averaged data on single levels from 1940 to present, https://doi.org/10.24381/cds.f17050d7, 2023.

Kim, H., Yeh, P. J. -F., Oki, T., and Kanae, S.: Role of rivers in the seasonal variations of terrestrial water storage over global basins, Geophysical Research Letters, 36, 2009GL039006, https://doi.org/10.1029/2009GL039006, 2009.

Ling, X., Huang, Y., Guo, W., Wang, Y., Chen, C., Qiu, B., Ge, J., Qin, K., Xue, Y., and Peng, J.: Comprehensive evaluation of satellite-based and reanalysis soil moisture products using in situ observations over China, Hydrol. Earth Syst. Sci., 25, 4209–4229, https://doi.org/10.5194/hess-25-4209-2021, 2021.

Rohde, M. M., Albano, C. M., Huggins, X., Klausmeyer, K. R., Morton, C., Sharman, A., Zaveri, E., Saito, L., Freed, Z., Howard, J. K., Job, N., Richter, H., Toderich, K., Rodella, A.-S., Gleeson, T., Huntington, J., Chandanpurkar, H. A., Purdy, A. J., Famiglietti, J. S., Singer, M. B., Roberts, D. A., Caylor, K., and Stella, J. C.: Groundwater-dependent ecosystem map exposes global dryland protection needs, Nature, 632, 101–107, https://doi.org/10.1038/s41586-024-07702-8, 2024.

Scanlon, B. R., Zhang, Z., Save, H., Sun, A. Y., Müller Schmied, H., van Beek, L. P. H., Wiese, D. N., Wada, Y., Long, D., Reedy, R. C., Longuevergne, L., Döll, P., and Bierkens, M. F. P.: Global models underestimate large decadal declining and rising water storage trends relative to GRACE satellite data, Proceedings of the National Academy of Sciences, 115, E1080–E1089, https://doi.org/10.1073/pnas.1704665115, 2018.

Wang, L. and He, Y.: Research on outlier threshold of automatic SoilMoisture observation data, meteorol. Mon., 41, 1017–1022, 2015.

Zeng, J., Yuan, X., Ji, P., and Shi, C.: Effects of meteorological forcings and land surface model on soil moisture simulation over China, J. Hydrol., 603, 126978, https://doi.org/10.1016/j.jhydrol.2021.126978, 2021.

Zeng, J., Yuan, X., and Ji, P.: The important role of reliable land surface model simulation in high-

resolution multi-source soil moisture data fusion by machine learning, J. Hydrol., 630, 130700, https://doi.org/10.1016/j.jhydrol.2024.130700, 2024.

Zeng, J., Yuan, X., Yang, H., Ji, P., and Xu, X.: Characterizing flash drought patterns in eastern China based on high-resolution and long-term soil moisture fusion data, J. Hydrol., 661, 133680, https://doi.org/10.1016/j.jhydrol.2025.133680, 2025.

Zhang, P., Zheng, D., van der Velde, R., Wen, J., Ma, Y., Zeng, Y., Wang, X., Wang, Z., Chen, J., and Su, Z.: A dataset of 10-year regional-scale soil moisture and soil temperature measurements at multiple depths on the tibetan plateau, Earth Syst. Sci. Data, 14, 5513–5542, https://doi.org/10.5194/essd-14-5513-2022, 2022.

Zhao, M., A, G., Zhang, J., Velicogna, I., Liang, C., and Li, Z.: Ecological restoration impact on total terrestrial water storage, Nat. Sustainability, 4, 56–62, https://doi.org/10.1038/s41893-020-00600-7, 2021.

Zomer, R. J., Xu, J., and Trabucco, A.: Version 3 of the global aridity index and potential evapotranspiration database, Sci. Data, 9, 409, https://doi.org/10.1038/s41597-022-01493-1, 2022.